

## Phase Transitions in $SO(3)$ Lattice Gauge Theory

Saumen Datta<sup>1,3</sup> and Rajiv V. Gavai<sup>1,2,4</sup>

<sup>1</sup>*Theoretical Physics Group,  
Tata Institute of Fundamental Research,  
Homi Bhabha Road, Mumbai-400005, India.*

<sup>2</sup>*Zentrum für interdisziplinäre Forschung,  
Wellenberg 1, D-33615 Bielefeld, Germany.*

### Abstract

The phase diagram of  $SO(3)$  lattice gauge theory is investigated by Monte Carlo techniques on both symmetric  $N_\sigma^4$  and asymmetric  $N_\sigma^3 \times N_\beta$  lattices with a view i) to understand the relationship between the bulk transition and the deconfinement transition, and ii) to resolve the current ambiguity about the nature of the high temperature phase. A number of tests, including an introduction of a magnetic field and measurement of different correlation functions in the phases with positive and negative values for the adjoint Polyakov line,  $L_a$ , lead to the conclusion that the two phases correspond to the same physical state. Studies on lattices of different sizes reveal only one phase transition for this theory on all of them and it appears to have a deconfining nature.

---

<sup>3</sup>E-mail:saumen@theory.tifr.res.in

<sup>4</sup>E-mail:gavai@theory.tifr.res.in

# 1 Introduction

The formulation of gauge theories on discrete space-time lattices [1] provide an elegant way to investigate confinement in nonabelian gauge theories. Using numerical Monte Carlo techniques, it was shown [2] that confinement survives the approach to continuum limit of  $a \rightarrow 0$ , where  $a$  is the lattice spacing. The same techniques enabled to explore these theories at nonzero temperatures where it was found [3] that both  $SU(2)$  and  $SU(3)$  Yang-Mills theories undergo deconfinement phase transitions to a new phase of deconfined glue. Exploiting the symmetry of their order parameters, it was argued [4] that the  $SU(3)$  theory should have a first order transition while the critical exponents of the  $SU(2)$  theory should be the same as those of the 3-dimensional Ising model, which was confirmed by high precision determination [5] of the exponents.

Since the continuum limit is at the critical point of a lattice theory, a large class of actions, which are in the same universality class as the popular Wilson action [1], given by eqn.(1),

$$S = \beta_f \sum_p \left\{ 1 - \frac{1}{N} \text{Re Tr}_f U_p \right\} , \quad (1)$$

are expected to give rise to the same predictions for the continuum physics. In particular, the trace, taken in the fundamental representation of the gauge group, in eqn.(1) can be taken in any representation of the gauge group. Indeed, as the 2-loop  $\beta$ -function for pure  $SU(2)$  gauge theory is identical to that of the pure  $SO(3)$  gauge theory, one expects the latter to yield the same physics of confinement and deconfinement. On the other hand,  $SO(3)$  does not have the  $Z(2)$  center symmetry whose spontaneous breakdown in the  $SU(2)$  theory indicates the deconfinement transition. This makes the investigation of the phase diagram of the  $SO(3)$  gauge theory especially interesting and important. It has been argued [6] that the deconfinement transition, in this case, will show up as a cross over which sharpens in the continuum limit to give the Ising-like second order phase transition.

Another reason for investigating the finite temperature transition in  $SO(3)$  gauge theory is that it is supposed [7] to have a bulk phase transition and may thus provide a test case for studying the interplay between the types of phase transitions. Recently, simulations of the Bhanot-Creutz action [7] for  $SU(2)$  gauge theory,

$$S = \sum_p \left\{ \beta_f \left( 1 - \frac{1}{2} \text{Tr}_f U_p \right) + \beta_a \left( 1 - \frac{1}{3} \text{Tr}_a U_p \right) \right\}. \quad (2)$$

at finite temperature revealed [8] that the known deconfinement transition point in Wilson action becomes a line in the  $\beta_f - \beta_a$  plane and joins the bulk transition line seen in [7]. The

order of the deconfinement transition was also seen to change from second to first for  $\beta_a \geq 1.25$ . At no  $\beta_a$ , two separate transitions were found in spite of variations in the lattice size in temporal directions from  $N_t = 2$  to 8. Considering the different physical nature of these transitions, their coincidence was puzzling. In view of the behaviour of the order parameter for the deconfinement phase transition, it was concluded in [9] that the transition seen in [7] is a deconfinement transition rather than a bulk one. However, very little shift in the transition coupling was seen under a change of  $N_t$ , which is more characteristic of a bulk transition.

The studies in [8, 9] were all done for a relatively small  $\beta_a$ , i.e., close to the Wilson action. In this paper we study the Bhanot-Creutz action with  $\beta_f = 0$  with an aim to study the issue of bulk vs deconfinement transitions away from the Wilson action axis. As the trace is then taken only in the adjoint representation, it corresponds to  $SO(3)$  gauge theory. Such a study of finite temperature  $SO(3)$  gauge theory was carried out in [10] and a deconfining transition for this theory was found. However, there was some ambiguity about the nature of the high temperature phase and the order of the phase transition in [10]. In this work, we attempt to clarify the nature of the high temperature phase, and the order of the phase transition for  $SO(3)$  lattice gauge theory.

The plan of our paper is as follows: in section 2, we define the actions and the different observables we use for our study. In section 3, we discuss the nature of the high temperature phase with a view to clarify some of the issues in [10]. Finite size scaling analysis is used in the next section to establish the order of the transition of  $SO(3)$  gauge theory. In section 5, the issue of bulk versus deconfinement transition is discussed. The last section contains a summary of our results and their discussion.

## 2 Actions and Observables

The Wilson action for  $SO(3)$  gauge theory is

$$S = \beta \sum_p \left(1 - \frac{1}{3} \text{Tr} U_p\right) \quad (3)$$

where  $U_p$  denotes the directed product of the basic link variables which describe the gauge fields,  $U_\mu(x) \in SO(3)$ , around an elementary plaquette  $p$ . Comparing the naive classical continuum limit of eqn. (3) with the standard action for  $SU(2)$  Yang-Mills theory, one obtains  $\beta = 3/2g_0^2$ , where  $g_0$  is the bare coupling constant of the continuum theory.

Using the property of the adjoint trace,  $\text{Tr}_a V = (\text{Tr}_f V)^2 - 1$ , the action (2) can be written

for  $\beta_f = 0$  as

$$S = \frac{4\beta_a}{3} \sum_p \left\{ 1 + \left( \frac{1}{2} \text{Tr}_f U_p \right)^2 \right\} . \quad (4)$$

This form is advantageous for numerical simulations, since one can use the Pauli matrix representation for the  $SU(2)$  matrices. It was found in [7] that this action has a first order bulk transition at  $\beta \sim 2.5$ . We have checked that the two actions above give identical results, and then used (4) for our simulations. Another action that we used is the Halliday-Schwimmer action [11]

$$S = \frac{\beta_v}{2} \sum_p \sigma_p \text{Tr}_f U_p . \quad (5)$$

Here  $U_p$  is defined as before but the link variables  $U_\mu(x) \in SU(2)$ , and  $\sigma_p = \pm 1$ . Besides the integration over the link variables, the partition function in this case also contains a summation over all possible configurations of the set  $\{\sigma_p\}$ , thus ensuring that the action is blind to the  $Z(2)$  center symmetry of  $SU(2)$ . It is thus as good as (3) for exploring the role of  $Z(2)$  in deconfinement transition. It was found in [11] that the action (5) shows a first order bulk phase transition at  $\beta_v \sim 4.5$ . The chief advantage of this action is that both the link variables  $U_\mu$  and the plaquette variables  $\sigma_p$  can be updated using heat-bath algorithms [2]. We have used it for both qualitative studies of nature of the high temperature phase in the next section and for quantitative investigations in later sections, where substantial computation was necessary.

One of the observables which we used to monitor the phase transitions is the adjoint plaquette variable  $P$ , defined as the average of  $\frac{1}{3} \text{Tr}_a U_p$  over all plaquettes for actions (3) and (4); for the action (5),  $P$  is defined as the average of  $\sigma_p \text{Tr}_f U_p$  over all plaquettes. The order parameter of the deconfinement transition in  $SU(2)$  gauge theory,  $\langle L_f \rangle$ , where  $L_f$  is given by,

$$L_f(\vec{r}) = \text{Tr}_f \prod_{i=1}^{N_t} U_t(\vec{r}, i) , \quad (6)$$

is identically zero for the actions (4) and (5) due to their local  $Z(2)$  symmetry. Its natural analogue for the  $SO(3)$  theory is  $\langle L_a \rangle$ , the average over all spatial sites of the adjoint Polyakov loop, defined by

$$L_a(\vec{r}) = \text{Tr}_a \prod_{i=1}^{N_t} U_t(\vec{r}, i) . \quad (7)$$

Note that  $\langle L_a \rangle$ , unlike  $\langle L_f \rangle$ , is not an order parameter, as it is not constrained to be zero in the confined phase. Since  $\langle L_a \rangle$  and  $\langle L_f \rangle$  can be thought of as measures of free energy of a fundamental and an adjoint quark respectively, their different behaviour in the confined phase is related to the fact that an adjoint quark in the confined phase can be screened by gluons created from the vacuum, while a fundamental quark cannot. For the same reason, an

adjoint Wilson loop is not supposed to exhibit the area law. However, creation of gluon pairs from vacuum costs a considerable amount of energy as glueballs are heavy. It may therefore be favourable for adjoint quarks also to have a string between them, at least when they are not too far separated. Intermediate size adjoint Wilson loops were found [12] to show an area law for  $SU(2)$  gauge theory, giving a string tension that is  $\sim 2$  times as large as the fundamental string tension. Furthermore, the behaviour of the adjoint Polyakov loop across the  $SU(2)$  deconfinement transition was found to be qualitatively similar to that of the fundamental Polyakov loop:  $\langle L_a \rangle \sim 0$  (for  $8^3 \times 2$  and  $8^3 \times 4$  lattices) till the deconfinement transition, where it acquires a nonzero value [13]. The jump in  $\langle L_a \rangle$  (and also in even higher representation Polyakov loops) is surprisingly similar to that in  $\langle L_f \rangle$ . This is believed to be related to opening of mass gap across deconfinement: below the deconfinement transition, adjoint quark can exist only by forming a bound state with gluon, which costs a lot of energy and leads to a small expectation value for  $\langle L_a \rangle$ .

For the same reason,  $\langle L_a \rangle$  can be expected to show a sharp change at the deconfinement transition for  $SO(3)$  gauge theory also and can, therefore, serve as a good indicator of deconfinement transition in  $SO(3)$  gauge theory. The behaviour of  $\langle L_a \rangle$  in finite temperature  $SO(3)$  gauge theory was studied numerically in Ref. [10]. Using a  $7^3 \times 3$  lattice and the action (4), it was found that  $\langle L_a \rangle$  was consistent with zero till  $\beta_a \sim 2.5$ , after which it became nonzero, indicating a deconfinement transition around this value of  $\beta_a$ .

### 3 The High Temperature Phase

An unexpected and curious result of Ref. [10] was that after becoming nonzero in the high temperature phase,  $\langle L_a \rangle$  settles into either a positive value ( $\rightarrow 3$  as  $\beta_a \rightarrow \infty$ ), or a negative value ( $\rightarrow -1$  as  $\beta_a \rightarrow \infty$ ), the average value of the action being the same for both the states. In [10] the negative  $\langle L_a \rangle$  state was interpreted as the manifestation of another zero temperature confined phase. Since its negative value is inconsistent with its being the exponential of the free energy of an adjoint quark, it was conjectured that the negative value is a finite volume effect and that it should go to zero on bigger lattices.

We have carried out a number of tests in order to understand the nature of the negative  $\langle L_a \rangle$  state. First, it was checked that the appearance of this phase is not due to any algorithmic problem, by checking that it appears irrespective of whether one uses action (3), (4) or (5). Since one uses explicitly  $SO(3)$  symmetric multiplication table for the first of these actions and a heat-bath for the third, any doubts of the negative  $\langle L_a \rangle$ -phase being an artifact of the  $SU(2)$ -based algorithm vanished when it was observed for all the three actions for the corresponding

Table 1:  $\langle L_a \rangle$  in the negative state for  $\beta_a = 3.5$  on  $N_s^3 \times 3$  lattices with  $N_s$  ranging from 7 to 18.

$N_s$	7	9	12	15	18
$\langle L_a \rangle$	-0.656(1)	-0.643(3)	-0.643(3)	-0.640(3)	-0.641(4)

deconfined phases. Indeed, unlike Ref. [10] or action (4), where only the hot starts in the deconfined phase lead to it, the heat-bath algorithm for the action (5) yielded it from even cold starts in the deconfined phase. Next, we checked whether the negative value is a finite size effect by simulating the theory on  $N_s^3 \times 3$  lattices with  $N_s$  ranging from 7 to 18. Our results are presented in table 1. They indicate that the value of  $\langle L_a \rangle$  is quite stable against change in spatial lattice size. Looking at the trend for  $N_s = 9$  to  $N_s = 18$  in table 1, one can estimate the value of  $\langle L_a \rangle$  to be  $\sim -0.64(1)$  on an  $\infty^3 \times 3$  lattice.

The constancy of  $\langle L_a \rangle$  in the negative phase above suggests it to be a genuine state on an  $\infty^3 \times N_t$  lattice. Just as the negative  $\langle L_f \rangle$ -phase of the  $SU(2)$  theory is physically the same as the positive  $\langle L_f \rangle$ -phase, the negative  $\langle L_a \rangle$ -phase could be similar to the positive  $\langle L_a \rangle$ -phase. A way to test this possibility is to introduce a polarising ‘magnetic field’ by adding a term  $h \sum_{\vec{x}} L_a(\vec{x})$  to the action (4). As shown in Fig. 1, the average plaquette  $\langle P \rangle$  on a  $7^3 \times 3$  lattice is not affected strongly by this term either below the transition ( $\beta_a = 2.3$ ) or above the transition ( $\beta_a = 3.5$ ). However,  $\langle L_a \rangle$  is. Irrespective of the starting configuration, it always converges to a unique value whose sign is determined by that of  $h$ , whereas for  $h = 0$  only some hot starts settled to negative  $\langle L_a \rangle$ . Defining  $\langle L_a \rangle$  as,

$$\langle L_a \rangle = \lim_{h \rightarrow 0^+} \lim_{V \rightarrow \infty} \frac{\partial}{\partial h} \ln Z(h) \quad , \quad (8)$$

in analogy with spin models, where one looks for a spontaneous breakdown of a symmetry in this way, one also gets a positive  $\langle L_a \rangle$  always. This too is similar to the  $SU(2)$  case, except that the normalizations of  $\langle L_a \rangle$  coming from the two different phases are different here, being 3 and 1 respectively. This suggests strongly that the high temperature phase of the  $SO(3)$  gauge theory also manifests itself in two ways corresponding to positive and negative  $\langle L_a \rangle$ . Also note

in Fig. 1 that the same definition of  $\langle L_a \rangle$  yields a value consistent with zero below the phase transition.

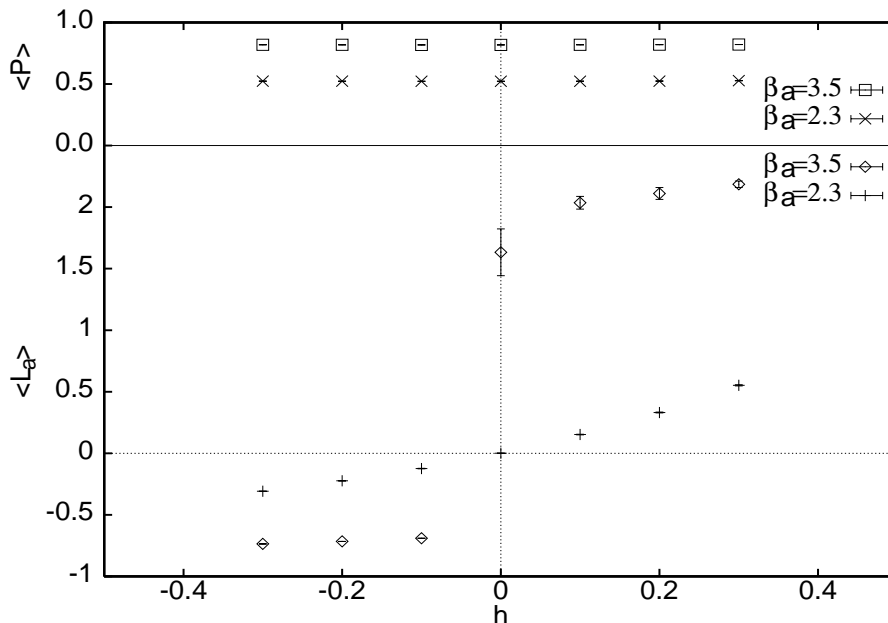


Figure 1:  $\langle P \rangle$  and  $\langle L_a \rangle$  for a  $7^3 \times 3$  lattice, for  $\beta_a = 2.3$  and  $3.5$ , in the presence of a magnetic field  $h$ .

A further test of the similarity of the physics in these two phases is provided by the correlation functions in these phases. If the phases are indeed physically similar, they ought to have the same correlation lengths, and therefore, the same correlation functions apart from normalisations. In fact, it has been argued [6] that even for the  $SU(2)$  theory the true order parameter is the two point correlation function of  $L_f$ . The behaviour of the two point correlator is known to be quite different in the confined and the deconfined phases. In the limit of infinite separation, it goes to zero in the confined phase and a constant in the deconfined phase. In Fig. 2 we show  $\Gamma(r)$  on an  $8^3 \times 4$  lattice, defined by

$$\Gamma(r) = \sum_i \sum_{\vec{x}} \langle L_a(\vec{x} + r\vec{e}_i) L_a(\vec{x}) \rangle \quad , \quad (9)$$

as a function of  $r$  in lattice spacing units for  $\beta_a = 2.3$  and for the positive and negative  $\langle L_a \rangle$  states at  $\beta_a = 2.6$  and  $3.5$ . At each  $\beta$  value  $5 \times 10^6$  iterations were made. The errors were calculated by dividing the measurements into blocks of 5000 each. It was checked that altering the bin-size does not change the error. For  $\beta_a = 2.3$ , the  $r=4$  point and the errors for the  $r=3$  point are not shown, as the former has a negative central value, being consistent with zero

within error, and the latter are of the order of the mean itself. One clearly sees that i) below the transition at  $\beta_a = 2.3$ , the correlator vanishes rapidly with  $r$ , ii) it approaches a constant above the phase transition and iii) the constant is bigger for larger  $\beta_a$  and bigger in the positive  $\langle L_a \rangle$ -phase for the same  $\beta_a$ .

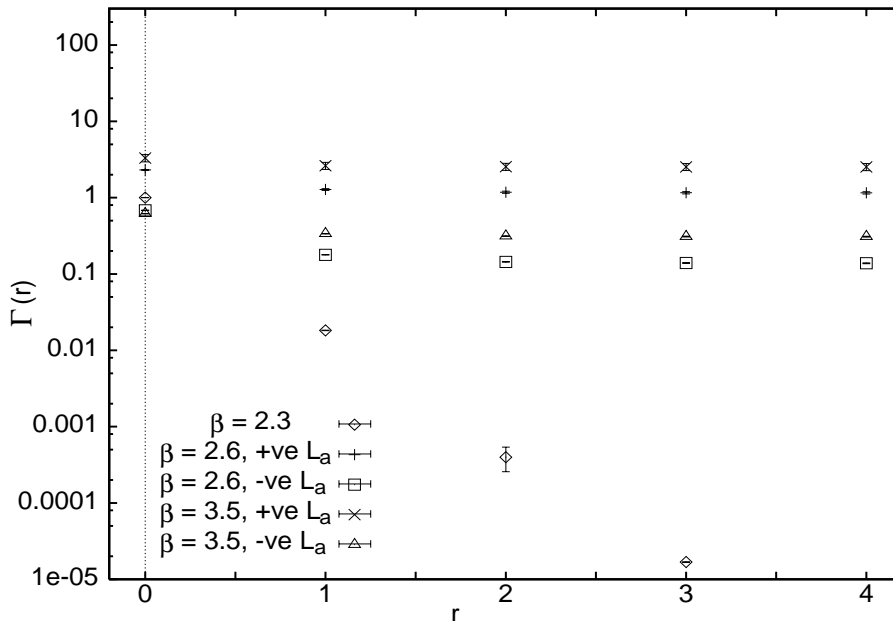


Figure 2: The two-point correlator  $\Gamma(r)$  plotted versus  $r$  on a  $8^3 \times 4$  lattice for  $\beta_a = 2.3, 2.6$  and  $3.5$

Finally, one can extract correlation lengths or mass gaps from these correlation functions on sufficiently large lattices. The mass gap can be obtained directly from the connected parts of the correlator above or from their zero momentum projected versions. Our intention here is only to compare the behaviour of the correlators in the low  $\beta$ -phase with that of the correlators in the two states of the high  $\beta$ -phase. Consequently, a small lattice should suffice as well; the mass gap so obtained will be influenced by higher states which should, however, be expected to be similar in the two high temperature phases. It was found that due to large fluctuations in  $L_a$ , the signals for connected part of the correlation function were difficult to extract. However, the signal improved considerably by looking at  $\Gamma(r-1) - \Gamma(r)$ , as shown in Fig. 3 (errors for  $r = 4$  are of the size of the correlation function itself and are not shown for clarity). As expected for states with same physics, the positive and negative  $\langle L_a \rangle$  states corresponding to both  $\beta_a = 2.6$  and  $3.5$  have a similar mass gap, which does not change significantly as one increases  $\beta_a = 2.6$  to  $3.5$ . The mass gap is, however, considerably different for  $\beta_a = 2.3$ . Interestingly, this picture

too matches well with the knowledge from  $SU(2)$  gauge theory, where it has been found that above the deconfinement transition, the mass gap changes very little with coupling [14].

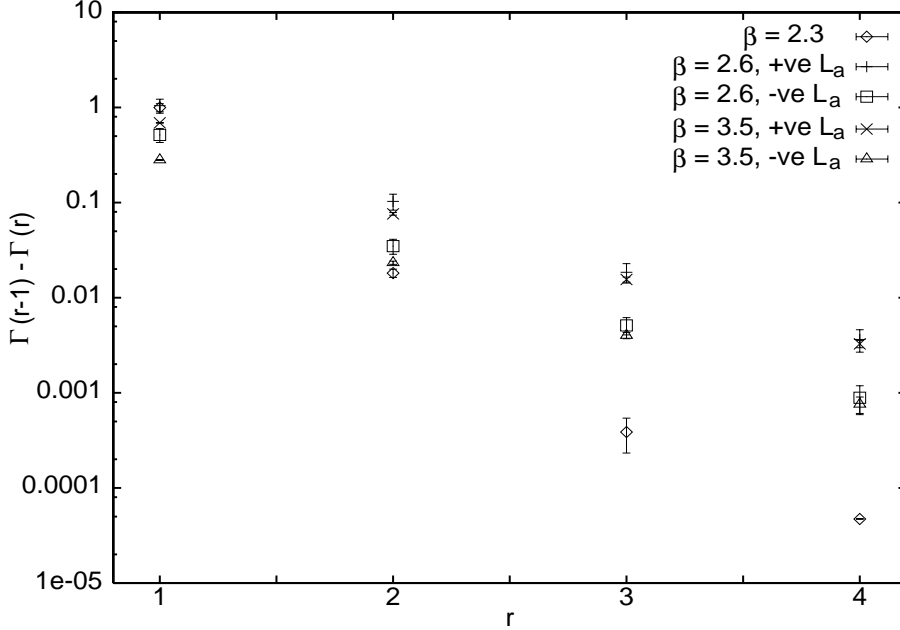


Figure 3:  $\Gamma(r-1) - \Gamma(r)$  vs.  $r$ , for  $\beta_a = 2.3, 2.6, 3.5$ .

Essentially the same conclusions emerge from the zero momentum correlators shown in Fig. 4. Defining the zero momentum projection by averaging the adjoint Polyakov loop over planes,

$$L_{ap}(x) = \sum_{y,z} L_a(x, y, z) \quad , \quad (10)$$

one defines its correlator in the usual way:

$$\Gamma_p(r) = \sum_x \langle L_{ap}(x+r) L_{ap}(x) \rangle \quad . \quad (11)$$

As is well known, a transfer matrix approach allows one to define the mass gap from the connected parts of these correlators and again we consider  $\Gamma_p(r-1) - \Gamma_p(r)$  to reduce fluctuations.

In summary, the effect of the external field  $h$  on the two phases of  $\langle L_a \rangle$  above the transition and the behaviour of the correlation functions in these phases suggest strongly that they are physically the same phases. Together with the corresponding results for the phase below the transition, they further suggest that the phase transition is a deconfining one and the high temperature phase appears either as a positive or equivalently as a negative  $\langle L_a \rangle$ -phase.

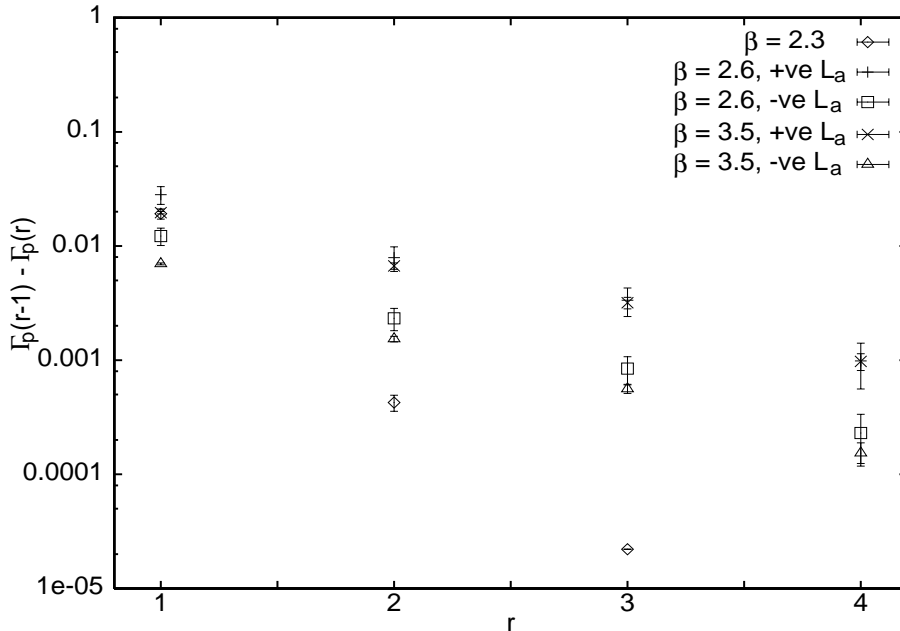


Figure 4: Variation of the subtracted plane-plane correlator,  $\Gamma_p(r-1) - \Gamma_p(r)$  with  $r$ . The values of couplings are 2.3, 2.6, 3.5.

## 4 Order of the Transition

In order to determine the order of the transition, simulations were made on  $4^3 \times 4$ ,  $6^3 \times 4$  and  $8^3 \times 4$  lattices with the action (5) and usual finite size scaling techniques were employed <sup>1</sup>.

Long lived metastable states were observed on all lattices near the transition region, signalling a possible first order transition. Runtime evolutions of the plaquette  $P$  and the Polyakov loop  $L_a$  from different starting configurations, averaged over bins of 50 iterations, are presented in Fig. 5 for the  $8^3 \times 4$  lattice. Runs on smaller lattices, not shown here, show more tunnellings and larger fluctuations in the positive  $L_a$ -phase but are otherwise similar in character. The  $L_a$  tunnels between all the three states, two of which correspond to the same value of the action but different signs of  $L_a$ . The transition point was estimated by demanding equal probability in the two phases for the action for these metastable states and error on it was estimated by observing a lack of tunnelling. For the  $4^3 \times 4$ ,  $6^3 \times 4$  and  $8^3 \times 4$  lattices the transition points are at  $\beta_{vc} = 4.43 \pm 0.02$ ,  $4.45 \pm 0.01$  and  $4.45 \pm 0.01$  respectively.

<sup>1</sup> Exploratory studies were also done for action (4) to check that they give similar results. Some of these results can be found in [15]. The only change in this case is that the transition occurs at  $\beta_a \sim 2.5$  [10, 15] but it displays the same features as discussed in this section for action (5).

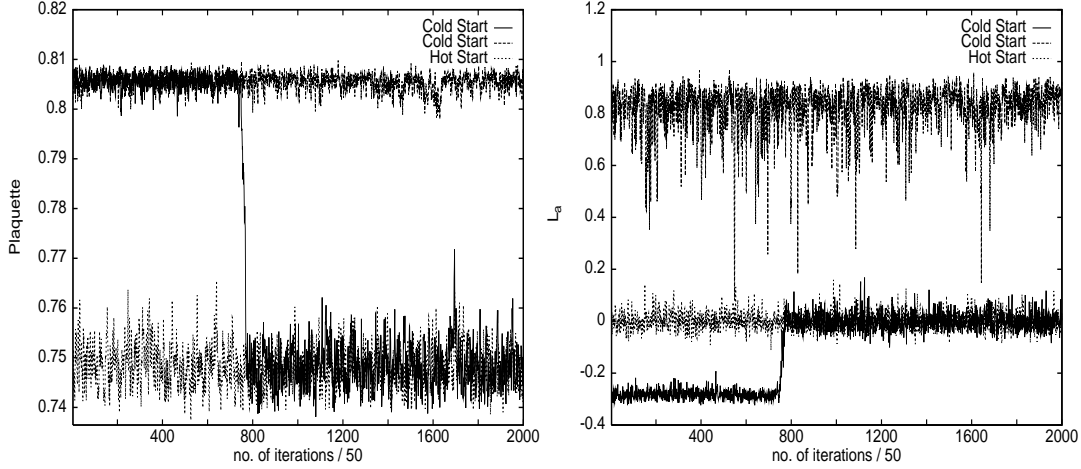


Figure 5: a) Runtime evolution of plaquette for  $8^3 \times 4$  lattice. The values have been binned over 50 iterations. b) Same for  $\langle L_a \rangle$ .

Table 2: The discontinuities in the plaquette  $\langle P \rangle$  and  $\langle L_a \rangle$  at the transition temperature on  $N_s^3 \times N_t$  lattices. The last two columns list the differences of  $\langle L_a \rangle$  in the two high temperature phases with that in the low temperature phase. The errors correspond to the bin size used.

$N_t$	$N_s$	$\beta_{vc}$	$\Delta P$	$\Delta L_{a+}$	$\Delta L_{a-}$
4	4	4.43	.0630(30)	.92(6)	-
4	6	4.45	.0575(30)	.86(4)	.26(2)
4	8	4.45	.0575(30)	.87(4)	.28(4)
6	6	4.45	.0575(30)	.42(4)	.13(4)
8	8	4.45	.0575(30)	.20(4)	.04(4)

In order to confirm the above indications of a first order transition in a more quantitative study, the distributions of the plaquette and  $\langle L_a \rangle$  were analysed. Fig. 6 displays the distributions of the plaquette variable on the lattices studied from the runs made at the critical couplings but from different starts. We performed about 100K-400K heat-bath sweeps depending on the size of the lattice. There is a clear two-peak structure in the distributions. While the position of one of the peaks shift slightly in going from  $4^3 \times 4$  to  $6^3 \times 4$  lattice, no shift is seen in going from  $6^3 \times 4$  to  $8^3 \times 4$  lattice. Assuming the peak positions to correspond to the expectation values in  $N_s \rightarrow \infty$  limit, the estimates of the discontinuities in the plaquette are presented in Table 2. Clearly, the plaquette discontinuity remains constant with increasing lattice size. As seen from Fig. 6, the valley between the peaks becomes steeper with increasing spatial size for the lattice, signalling again a first order transition. The corresponding distributions for the Polyakov loop  $L_a$  are presented in Fig. 7, and the estimates of the discontinuity for both the positive and negative  $L_a$  phases are also given in Table 2. While the frequent tunnelling smoothens the peak structure for the  $4^3 \times 4$  lattice considerably, a clear three-peak structure is seen for both the  $6^3 \times 4$  and the  $8^3 \times 4$  lattices. Once again the peak positions are seen not to shift and the valley between peaks is seen to become steeper with increasing lattice size, pointing to a finite discontinuity in the infinite volume limit and a first order transition. It is also interesting to note that the peak for the confined phase is almost precisely at zero. As argued in Section 2, one expects to see a linearly rising potential between static adjoint quarks in the confined phase of the  $SO(3)$  theory for intermediate distances. The leading order strong coupling contribution to  $\langle L_a(\vec{r})L_a(\vec{0}) \rangle$ ,  $\propto \exp(-V(r, T)/T)$ , is  $\beta^{rN_t}$  for a set of plaquettes spread between the loops, and  $\beta^{8N_t}$  for tubes around the loops. Thus if one is still in the leading order strong coupling regime at  $\beta_v = 4.45$ , one expects to see a linearly rising potential for lattice distances up to 8. This may explain  $\langle L_a \rangle = 0$  in the confined phase. We have, however, checked that even on a  $16^3 \times 4$  lattice it continues to remain zero and the histograms in Figs. 6 and 7 do not shift at all but become sharper and narrower.

## 5 Nature of the Transition

As mentioned in the Introduction,  $SO(3)$  lattice gauge theory is supposed to have a bulk transition [7, 11], while we argued above that the only transition seen on  $N_t = 4$  lattices is more appropriately identified as the deconfinement phase transition at high temperatures. In this section we attempt to address the issue of bulk transition.

Since the deconfinement temperature is a physical quantity (in the hypothetical world of gluons of 2 colours), it is expected to remain constant under a change of  $N_t$ :  $T_c = 1/N_t a(\beta_c)$

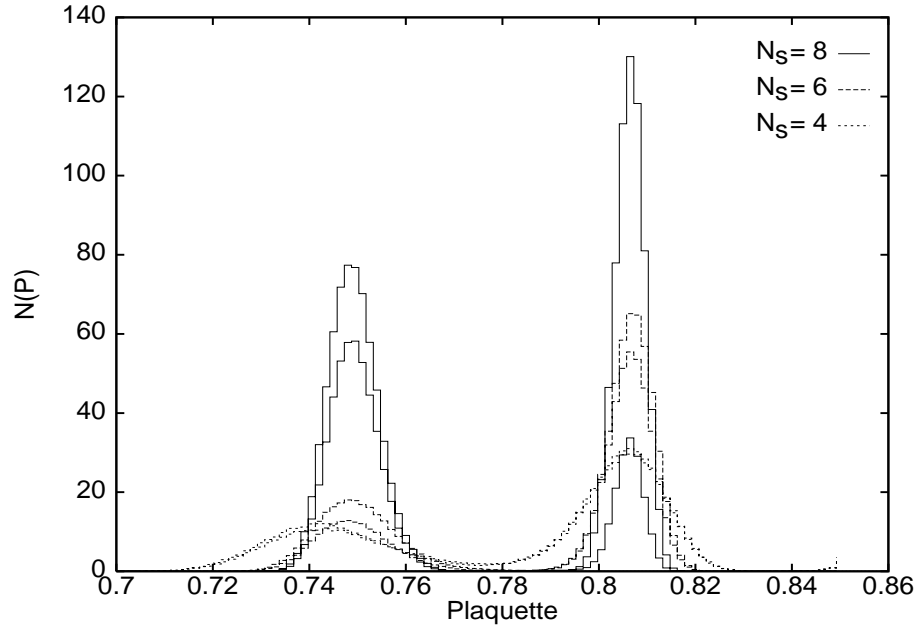


Figure 6: The distribution of the plaquette on  $N_s^3 \times 4$  lattices at the critical couplings given in Table 2.

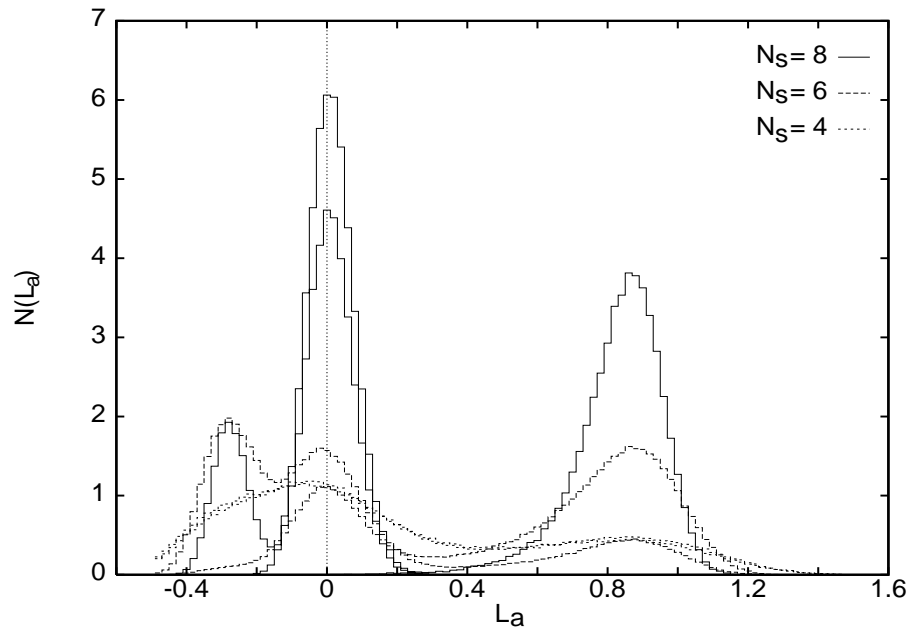


Figure 7: Distribution of  $L_a$  on  $N_s^3 \times 4$  lattices for couplings of Table 2.

Table 3: The critical coupling  $\beta_c$  as a function of the lattice size in the time direction, for the actions (4) and (5). Also presented are the corresponding values of  $\beta_c$  for pure  $SU(2)$  gauge theory with the action (1) (taken from [16]).

	$SO(3)$	$SO(3)$	$SU(2)$
$N_t$	action (5)	action (4)	action (1)
2	4.156(10)	2.415(5)	2.1768(30)
4	4.43(2)	2.53(1)	2.2986(6)
6	4.45(2)	2.52(2)	2.4265(30)
8	4.45(2)	2.52(2)	2.5115(40)

implies that a change in  $N_t$  should merely change  $\beta_c$  and push it to larger  $\beta$  as  $N_t$  is increased. In order to check this, we studied the theory on  $8^3 \times 2$ ,  $4^4$ ,  $6^4$  and  $8^4$  lattices. On all these lattices, only one transition point were found, where both the plaquette and  $\langle L_a \rangle$  show a discontinuity. The critical couplings for  $N_t = 2, 4, 6, 8$ , extracted from the runs made on the lattices above are presented in Table 3. We have also included in the table the corresponding critical couplings for action (4) from our own work and those for the deconfinement transition in  $SU(2)$  gauge theory, taken from Ref. [16].

It is found from Table 3 that as one goes from  $N_t = 2$  to  $N_t = 4$ , there is a clear shift in  $\beta_c$  in all the three cases. This behaviour is consistent with the deconfinement scenario. However, no perceptible change in  $\beta_c$  was found for either of the actions for  $SO(3)$  in going from  $N_t = 4$  to 6 and 8. This is in sharp contrast to the  $SU(2)$  case, and is also unexpected for a deconfinement transition. The distributions for the plaquette  $P$  are exhibited in Fig. 8. They again suggest a first order phase transition and the estimated discontinuity in plaquette is listed in Table 2. One sees that it remains constant as one increases  $N_t$ . We have also looked at the corresponding distributions of  $\langle L_a \rangle$  for these lattices. In spite of the noisy signals due to small spatial sizes a three-peak structure could still be ascertained in all of them. Table 2 lists the corresponding discontinuities for  $\langle L_a \rangle$ . It should be noted that  $\langle L_f \rangle$  at the transition point decreases with  $N_t$  for both  $SU(2)$  and  $SU(3)$  theories. The decrease in the discontinuities in  $\langle L_a \rangle$  in Table 2 are for similar reasons.

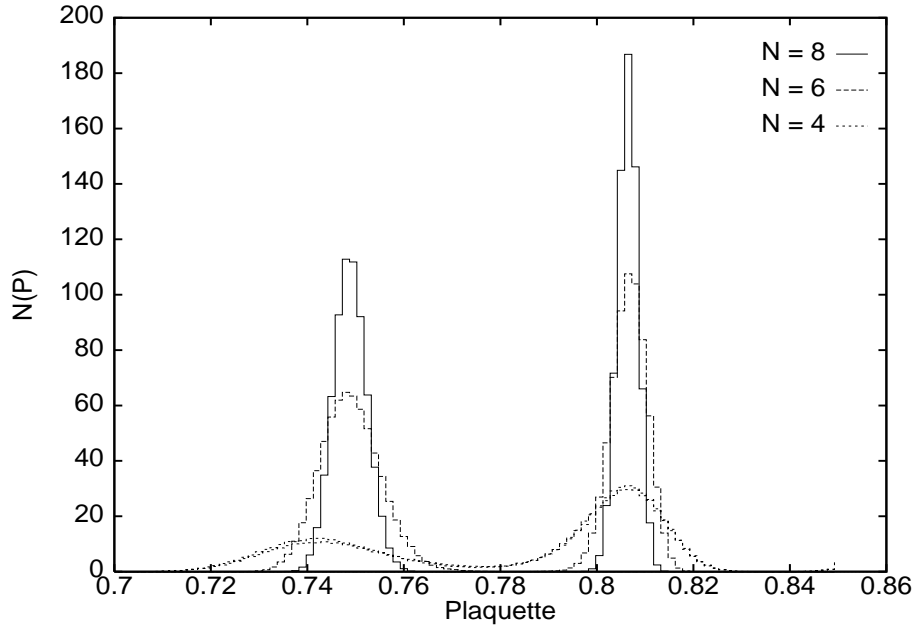


Figure 8: Distributions of the plaquette on  $N^4$  lattices at the critical couplings given in Table 2.

## 6 Summary and Discussion

The study of phase transitions in  $SO(3)$  gauge theory is important for understanding both the interplay of the bulk and the deconfinement transition, and the nature of its deconfinement as it has no center symmetry. The theory was studied in Ref. [10] on a  $7^3 \times 3$  lattice and a deconfining phase transition at  $\beta_{ac} \sim 2.5$  was reported. For  $\beta_a > \beta_{ac}$ ,  $\langle L_a \rangle$  was found to take either a positive value or a negative value. The positive  $\langle L_a \rangle$  state was taken to correspond to the high temperature deconfined phase while the negative  $\langle L_a \rangle$  state was interpreted as being another zero temperature confined phase.

Our simulations with a variety of actions confirmed the results of Ref. [10]. In particular, the negative  $\langle L_a \rangle$ -state was present in all of them. However, using a ‘magnetic field’ term to polarise, we found a unique  $\langle L_a \rangle$  state depending on the sign of the field. The correlation function measurements in both the phases of positive and negative  $\langle L_a \rangle$  also indicated that the two states are physically identical. Both of these correspond to the high temperature deconfined phase of  $SO(3)$  gauge theory, as the correlators approached a nonzero constant in the large separation limit, while below the transition a confined phase was indicated by their exponential drop to zero.

By studying the system on lattices of different sizes, it was established that there is only one phase transition for this theory, which is of first order. In addition to the average action, the adjoint Polyakov loop also showed a jump across the transition. Its vanishing until the transition point further supports the interpretation of a deconfining transition. The correlation lengths below and above  $\beta_c$  behave similar to the correlation lengths near the deconfinement transition of  $SU(N)$  gauge theories. If the transition is accepted to be a deconfinement phase transition then the first order nature of the transition is very puzzling, as the  $SU(2)$  gauge theory is known to have an Ising model-like second order phase transition.

On increasing  $N_t$  from 4 to 6 and 8, the transition point did not move. While investigations on still larger lattices will be required to conclude firmly, this observed behaviour does go against the usual expectations of a deconfinement transition, and suggests its interpretation as a bulk transition. Since we did not find any other transition, one is lead to accept either a coincident deconfinement transition or a total lack of a deconfinement phase transition for  $SO(3)$  gauge theory. If it is the former then it is remarkably similar to the results for the mixed action [8, 9], where too a shift in  $\beta_c$  was observed only in going from  $N_t=2$  to 4 for large  $\beta_a$  and suggests that very large lattices are necessary to see the similarity of  $SO(3)$  and  $SU(2)$  theories at finite temperature, if at all. The other alternative is clearly in disagreement with the naive expectations of purely gluonic confinement for  $SO(3)$  gauge theory.

## 7 Acknowledgements

We thank Dr. Srinath Chelubaraja and Dr. Sourendu Gupta for many helpful discussions. It is a pleasure for one of us (R. V. G.) to thank Profs. Frithjof Karsch and Helmut Satz and the staff at the Zentrum für interdisziplinäre Forschung, Universität Bielefeld for their kind hospitality.

## References

- [1] K. Wilson, *Phys. Rev.* **D10** (1970) 2445.
- [2] M. Creutz, *Phys. Rev.* **D21** (1980) 2308.
- [3] R.V. Gvai, in “Quantum Fields on the Computer”, Ed. M. Creutz, (World Scientific, 1992) p 51.
- [4] B. Svetitsky, *Phys. Rep.* **132** (1986) 1.

- [5] J. Engels, J. Fingberg and M. Weber, *Nucl. Phys.* **B332** (1990) 737.
- [6] A.V. Smilga, *Ann. Phys.* **234** (1994) 1.
- [7] G. Bhanot and M. Creutz, *Phys. Rev.* **D24** (1981) 3212.
- [8] R.V. Gavai, M. Grady and M. Mathur, *Nucl. Phys.* **B423**, 123 (1994).
- [9] R.V. Gavai and M. Mathur, *Phys. Rev.* **D56** (1997) 32; *Nucl. Phys.* **B448** (1995) 399.
- [10] S. Chelubaraja and H.S. Sharatchandra, hep-lat/9611001.
- [11] I.G. Halliday and A.Schwimmer, *Phys. Lett.* **B101** (1981) 327.
- [12] C. Bernard, *Nucl. Phys.* **B219** (1983) 341.
- [13] P. Damgaard, *Phys. Lett.* **B194**, 107 (1987).
- [14] U. M. Heller, F. Karsch and J. Rank, *Phys. Lett.* **B355** (1995) 511.
- [15] Saumen Datta and R.V. Gavai, in : Proceedings of the International Conference On Physics and Astrophysics of Quark-Gluon Plasma, Jaipur, 1997, to be published.
- [16] J. Fingberg, U. Heller and F. Karsch, *Nucl. Phys.* **B392** (1993) 493.